1998

# Detailed Numerical Simulation of Condensers and Evaporators Using Pure and Mixed Refrigerants

O. Garcia-Valladares
*Universitat Politecnica de Catalunya*

C. D. Perez-Segarra
*Universitat Politecnica de Catalunya*

J. Rigola
*Universitat Politecnica de Catalunya*

A. Oliva
*Universitat Politecnica de Catalunya*

# *DETAILED NUMERICAL SIMULATION OF CONDENSERS AND EVAPORATORS USING PURE AND MIXED REFRIGERANTS*

***O.García-Valladares, C.D.Pérez-Segarra, J.Rigola, A.Oliva***

Laboratori de Termotècnia i Energètica
Dept. Màquines i Motors Tèrmics. Universitat Politècnica de Catalunya
Colom 9, 08222 Terrassa (Barcelona), Spain
FAX: +34-93-7398101; Tel. +34-93-7398192
E-mail: labtie@termo1.mmt.upc.es

## *ABSTRACT*

A detailed one-dimensional numerical simulation of the thermal and fluid-dynamic behaviour of pipe condensers and evaporators has been developed. The discretized governing equations are coupled using two different algorithms: a step by step method and a pressure-based method of SIMPLE-like. A special treatment has been implemented in order to consider gas-liquid transitions. All the flow variables (temperatures, pressures, mass vapour fraction, gas and liquid velocities, heat fluxes, etc.) are evaluated at each point of the grid in which the domain is discretized. Local thermophysical properties are used. For both methods, different aspects such as complex geometry configurations (network of passages) and the influence of new non-contaminant refrigerants (pure refrigerants and mixtures) can be taking into account. Different numerical aspects together with some illustrative numerical results have been presented using R134a, iso-butane and R404A (ternary mixture) as refrigerant fluids.

## *NOMENCLATURE*

| | |
|---|---|
| CV | control volume |
| e | specific energy ($h + v^2/2 + gz\sin\theta$) |
| $f$ | friction factor |
| g | acceleration due to gravity |
| h | enthalpy. |
| $m$ | mass |
| $\dot{m}$ | mass flux |
| p | pressure |
| $\dot{q}$ | heat flux |
| S | cross section area |
| t | time |
| T | temperature |
| $x_g$ | mass fraction (vapour quality) |

| | |
|---|---|
| *Greek letters* | |
| $\alpha$ | heat transfer coefficient |
| $\delta$ | rate of convergency |
| $\varepsilon_g$ | void fraction |
| $\nu$ | velocity |
| $\theta$ | angle |
| $\tau$ | shear stress |
| $\zeta$ | roughness |
| *Subscripts* | |
| g | gas or vapour |
| l | liquid |
| onb | onset nucleate boiling |
| sat | saturation |

## *INTRODUCTION*

In household refrigerators and freezers the evaporators are sealed together forming complicated integral passages. When the flow is divided into different passages, the mass flow through each one of them is strongly dependent on the pressure drop, which is consequence of the global thermal and fluid-dynamic behaviour of the whole equipment. General, accurate and flexible methods are required for the design and optimization of these units, in order to take into account different aspects such as: the specific geometric characteristics (network of passages), the use of new non-contaminant refrigerants (pure substances and mixtures), etc.

In this paper a detailed one-dimensional numerical simulation of the thermal and fluid-dynamic behaviour of condensation and evaporation flow inside ducts has been developed. The discretized governing equations are coupled using two different algorithms:

- A fully implicit step by step method (in which the continuity, momentum and energy equations are solved together at each control volume in the flow direction)[1,2]. In case of complex passages and/or when the inlet and outlet pressure are specified, the inlet mass flow rate is iteratively estimated using a Newton Raphson algorithm.
- A fully implicit segregated pressure-based method of SIMPLE-like[3,4] based on the sequential resolution of the above mentioned governing equations in the whole domain. Convective terms are treated using first and higher order numerical schemes (central difference, smart, quick, etc).

The mathematical formulation requires the use of empirical information for the evaluation of heat transfer coefficients, shear stresses, void fractions a pressure drop through singularities. Different semi-empirical correlations have been selected for both cases of condensation and evaporation and considering pure substances and mixtures. A special treatment has been implemented in order to consider vapour-liquid transitions. The refrigerants properties are evaluated using the REFPROP[5] properties program.

## *MATHEMATICAL FORMULATION*

In this section the mathematical formulation of the two-phase flow inside a characteristic control volume of a duct (single-phase flow, liquid or gas, represents a particular case) is presented (for more details see reference 1). The mathematical formulation of the fluid flow is made neglecting the difference of the liquid and vapour temperatures in the subcooled boiling and post-dryout regime in the evaporating flow. Their effects are considered through the use of empirical correlations for the evaluation of the shear stress, the convective heat transfer and the flow structure, adequate to the flow patterns produced.

Assuming one dimensional flow and negligible axial heat conduction, the integrated continuity, momentum and energy conservation equations over a finite control volume (see figure 1), without considering second order terms, have the form[1]:

$$\dot{m}_i = \dot{m}_o + \frac{\partial m}{\partial t} \qquad (1)$$

$$(p_i - p_o)S - \tau P\Delta z - mg\sin\theta = \dot{m}_{g,o}v_{g,o} - \dot{m}_{g,i}v_{g,i} + \dot{m}_{l,o}v_{l,o} - \dot{m}_{l,i}v_{l,i} + \Delta z\frac{\partial \dot{m}}{\partial t} \qquad (2)$$

$$\bar{q}P\Delta z = \dot{m}(e_{l,o} - e_{l,i}) + \dot{m}_{g,o}(e_{g,o} - e_{l,o}) - \dot{m}_{g,i}(e_{g,i} - e_{l,i}) + (\bar{e}_g - \bar{e}_l)\frac{\partial m_g}{\partial t} + m_g\frac{\partial \bar{e}_g}{\partial t} + m_l\frac{\partial \bar{e}_l}{\partial t} - S\Delta z\frac{\partial \bar{p}}{\partial t} + (\bar{e}_l - \bar{e})\frac{\partial m}{\partial t} \qquad (3)$$

In the momentum equation, eq. (2), the evaluation of the shear stress is done by means of a single or two-phase friction factor $f$, which is usually calculated using empirical correlations. This factor is defined from the expression: $\tau = (f/4)(m^2/2\rho S^2)$. When a singularity is presented (sudden enlargement or sudden contraction), the single or two-phase pressure drop is calculated by means of a balance over an appropriate control volume assuming isentropic flow behaviour from the inlet section to the vena contracta (in the case of sudden contraction) and equal back face pressure and plenum pressure. In order to relate the convective heat transfer and the wall temperature, a convective heat transfer coefficient $\alpha$ is introduced, which is defined from the equation: $q = \alpha(T_{wall} - T_{fluid})$.

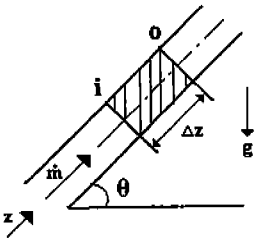

Figure 1

## *NUMERICAL SOLUTION*

In this section the main features related to the numerical solution of two-phase flow inside ducts using the step-by-step and the segregated pressure-based methods will be presented. The numerical simulation allows the detailed evaluation of the pressures, temperatures, velocities, void fractions, heat fluxes, etc. along the ducts. In both cases the domain is divided into control volumes (see figure 2). For each control volume, a set of algebraic equations is obtained by a discretization of the governing equations.

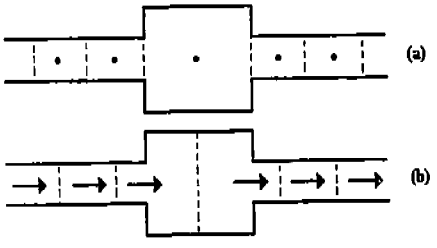

Figure 2. (a) Main grid nodes and their control volumes; (b) staggered location for mass fluxes and their control volumes

*Step-by-step method*

The flow is evaluated on the basis of a numerical implicit scheme. In each control volume (figure 2a), the values of the flow variables at the outlet section of each control volume are obtained by solving the resulting set of algebraic equations (continuity, momentum, energy and state equations) from the known values at the inlet section. The solution procedure is carried out in this manner, moving forward step by step in the flow direction[1]. At each cross section, the shear stresses, the convective heat fluxes and the void fractions are evaluated from empirical correlations obtained from the available literature (see next paragraph). The transitory solution is made every time step $\Delta t$. Depending on the time evolution of the boundary conditions, a constant or variable value of $\Delta t$ can be selected. The solution scheme requires the knowledge of values of the flow variables in the tube inlet as boundary conditions. Cases with boundary conditions of the type ($p_{in}$,$p_{out}$), ($p_{in}$, $\dot{m}_{out}$) or ($\dot{m}_{in}$, $p_{out}$) are iteratively solved using a Newton-Raphson algorithm. For more details see reference 2.

Figures 3 and 4 schematically show a case of single tube (with inlet and outlet regions) and a set of tubes forming parallel paths. In the latter case, the inlet mass flux through each tube, which is strongly dependent on the pressure drop, is iteratively evaluated by means of a Newton-Raphson algorithm.

*Pressure-based method (SIMPLEC)*

A variant of the SIMPLE method by Patankar and Spalding[3], called SIMPLEC[4], has been employed. The governing equations (1) to (3) are discretized by means of an implicit control-volume formulation. The domain is divided in a set of main control volumes (see figure 2a). For each control volume a grid node is assigned at its center. The different scalar variables (enthalpy, pressure and density) are calculated at each node of the main grid. Velocities are determined at the faces of these control volumes using staggered control volumes (figure 2b). This procedure not only avoids decoupling between continuity and momentum equations, but is also an excellent way to treat the discontinuities introduced by the flow geometry (contractions or expansions).

Convective terms are numerically approximated using the first-order upwind scheme and higher order schemes (central difference, smart, quick, ...); to avoid stability problems these terms are introduced as a deferred correction approach. At each grid node, enthalpy is obtained from the energy equation. Mass fluxes are calculated in their staggered locations from the momentum equation (together with the equation for the singularity when it is presented). Pressures are computed at the grid nodes using a pressure correction eq.; this equation is obtained from the continuity eq. using a corrected mass flux. All termophysical properties are evaluated at their local conditions.

The complete set of discretized momentum, energy and pressure-correction equations are solved by the direct TDMA Algorithm[3]. When the piping system includes parallel paths, the set of discretized equations is iteratively solved using TDMA along each path. Boundary conditions of the kind indicated above for the step-by-step method can be directly introduced.


Figure 3. Parallel paths.

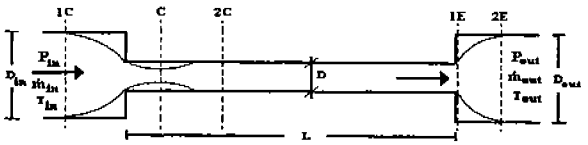


Figure 4. Single parallel path.

*Convergence criteria*

The convergence of the different iterative loops is considered to have reached when $|h-h^*|<\delta \cdot h_{in}$, $|p-p^*|<\delta \cdot p_{in}$ and $|\dot{m}-\dot{m}^*|<\delta \cdot \dot{m}_{in}$ is verified at each control volume. The superscript * indicates the value of the variable at the previous iteration and $\delta$ is the imposed precision. Global mass balances are also tested, specially when the step by step method is applied in complex geometries.

*Differentiation between regions*

The differentiation between the three main regions existing in both the condensation and the evaporation processes is given by the temperature, pressure and vapour quality. These conditions are: ***i)*** liquid region: $T<T_{sat}$, $p>p_{sat}$, $x_g=0$; ***ii)*** two-phase region: $T=T_{sat}$, $p=p_{sat}$, $0<x_g<1$, ***iii)*** vapour region: $T>T_{sat}$, $p<p_{sat}$, $x_g=1$. In the evaporation process, two more regions are presented: ***iv)*** subcooled boiling region: $(T_{wall}-T_{sat}) > (T_{wall}-T_{sat})_{onb}$, $p>p_{sat}$, $x_g=0$, ***v)*** post-dryout region: $T=T_{sat}$, $p=p_{sat}$, $x_{gd}<x_g<1$.

Using the conditions of differentiation between regions mentioned above, the control volume where transition occurs is detected. In order to evaluate the position of the transition point, two criteria have been considered[1]: ***i)*** *Transition criterion 1:* the transition point is assigned to the outlet section of the control volume (assignation to the inlet section or to the middle section would be equivalent criteria); ***ii)*** *Transition criterion 2:* the control volume is divided into two control volumes. The length of the first control volume is calculated from the energy equation, imposing saturated conditions with $x_g=0$, $x_g=x_{gd}$ or $x_g=1$ at the outlet section or $(T_{wall}-T_{sat})=(T_{wall}-T_{sat})_{onb}$. The length of the second one is calculated by simple difference. The numerical results here presented have been obtained using the *criterion 1* for the pressure-based method and the *criterion 2* for the step by step method.

## *EVALUATION OF THE EMPIRICAL COEFFICIENTS*

*Single-phase and condensing flow*

In the *single-phase regions* the convective heat transfer coefficient is calculated using the Nusselt and the Gnieliski[6] equations, for laminar and turbulent regimes respectively. The friction factor is evaluated from the expressions proposed by Churchill (cited by Lin et al.[7]).

In the *two-phase region* the convective heat transfer coefficient is calculated using the Dobson et al[8] correlations that employed two different expressions for the annular and wavy flow. The expression proposed by Soliman[9] for the Froude number is taken as a differentiation criterion between annular and wavy condensation. The void fraction is estimated from the semi-empirical equation by Premoli (cited by Rice[10]). The friction factor is calculated from the same eq. as in the case of the single-phase flow using a correction factor according to Friedel[11].

For *refrigerants mixtures* the same correlations mentionated above have been used. The convective heat transfer coefficent in the two-phase region is calculated using Dobson[8] correlation that is applicable to refrigerants mixtures using the mixtures refrigerants properties.

*Evaporating flow*

In the case of *subcooled boiling*, the convective heat transfer coefficient and the friction factor are treated separately. For the convective heat transfer, the beginning of the subcooled boiling is estimated according to Frost and Dzakowic[12]. The method proposed by Bergles and Rohsenow[13] is used to consider the transition between pure liquid convection heat transfer and boiling heat transfer, which is evaluated from the correlation proposed by Forster and Zuber[14]. The friction factor , the point of net vapour generation is estimated according to Saha and Zuber[15]; the friction factor is estimated from the single-phase expressions cited above, with a two-phase Reynolds number evaluated from the homogeneous flow model described by Hewitt[16] and the two-phase viscosity proposed by McAdams (cited by Hewitt[16]), and considering the real vapour fraction proposed by Levy[17].

In the *two-phase region*, before the point of dryout, the convective heat transfer is evaluated using the expression proposed by Chen[18]. The friction factor and the void fraction are calculated in the same way as in the condensation two-phase flow. The *post-dryout regime* is considered to begin at $x_{gd}$=0.9 for refrigeration purposes. The convective heat transfer has been evaluated from the correlation developed by Groeneveld[19]. The void fraction is evaluated using the homogeneous model. The friction factor is evaluated using the single-phase expressions mentioned above, using the two-phase viscosity proposed by McAdams.

For *mixtures* the same correlations use for pure refrigerant have been employed, except for the calculation of the heat transfer coefficient. In this case the correlation proposed by Jung and Radermacher[20] has been used.

*Singularities*

The pressure drop in a sudden contraction is evaluated using the homogeneous model equations (see, e.g., Hewitt and Hall-Taylor[21]); the contraction coefficient is evaluated using the classical Weisbach values. In a sudden enlargement an alternative expression for the pressure change proposed by Chisholm[22] has been used because the homogeneous model overpredict the rise in static pressure over an enlargement.

## *NUMERICAL RESULTS*

Based on the geometries presented in figures 3 and 4, different cases will be presented to show the influence of some numerical aspects (number of grid nodes, convective numerical schemes,...) and some fluid parameters (kind of fluid, geometry,....).

*Case 1*. A comparison of four different schemes: upwind (uds), central difference (cds), quick and smart using different number of CVs (25, 50, 200 and 300) and the pressure-based method is shown in figure 5 for a condensation inside an isothermal tube. The results corresponds to a single tube (fig. 4) with the following data: *i)* geometry: D=10mm, L=3m, $\theta$=0, $\zeta$=1.5·10$^{-6}$; *ii)* fluid: R134a; *iii)* tube boundary conditions: $T_{wall}$=45°C, *iv)* inlet fluid (z=0) boundary conditions: $T_{in}$=60°C, $p_{in}$=14.7 bar and $\dot{m}_{in}$=9 kg/h.

Figure 5a and 5b show the temperature distribution using 25 and 50 CVs; with 200 control volumes or more the differences between the different schemes are not appreciable. Higher accuracy is obtained with the quick/smart schemes. Figure 5c shows the influence of the number of grid nodes using the smart scheme.

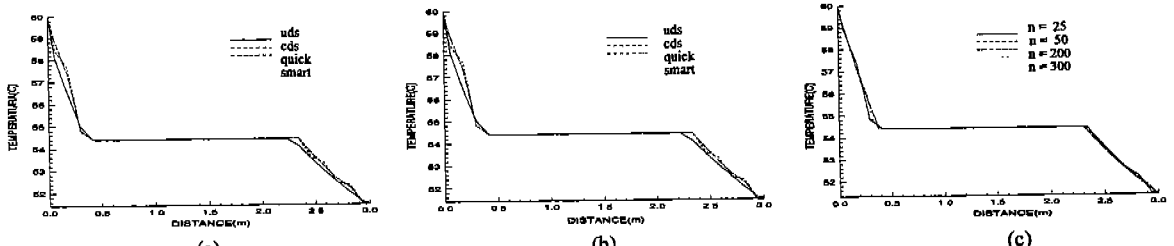


(a) (b) (c)

Figure 5. Influence of the numerical scheme and the number of control volumes. (a) 25 CVs, (b) 50 CVs, (c) smart with diffferent CVs

*Case 2*. Figure 6 shows a comparison between the step by step and the pressure-based methods (using smart) considering different number of control volumes. The same geometry, fluid and boundary conditions as the ones indicate in case 1 have been used. The differences between both methods are principally due to the transition criterion used in each one. With the second criterion, more accurate results are obtained for a given grid, or alternatively fewer control volumes are required for a given accuracy. This is in large measure due to the discontinuities presented in the empirical correlations between the different regions (see figures 7c and 8c).

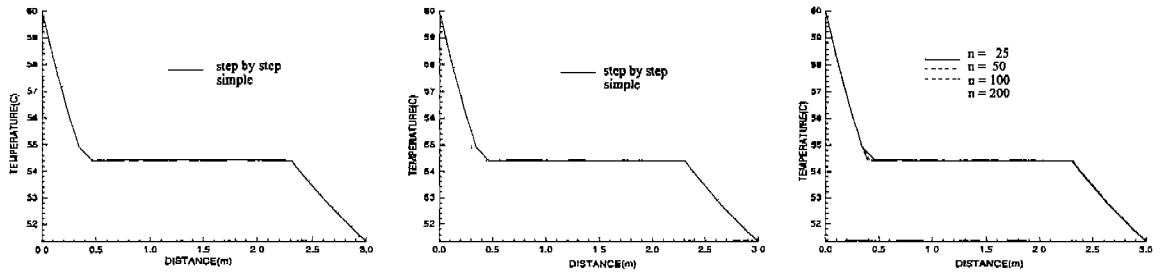


(a) (b) (c)

Figure 6. Step by step vs pressure-based methods (using smart) for two grids (a) 25 CVs and (b) 50 CVs; (c) step by step with different grids

*Case 3*. Condensation inside a branch with a sudden contraction in the inlet and a sudden enlargement in the outlet (fig. 4) using three different fluids. Input data: *i)* geometry: $D_{in}=D_{out}=5$ mm, D=3 mm, L=3 m, $\theta=0$, $\zeta=1.5\text{x}10^{-6}$; *ii)* fluids: R134a, R600a (isobutane) and R404A; *iii)* tube wall boundary conditions: $T_{wall}=45^{\circ}C$; *iv)* inlet fluid conditions (z=0): $T_{in}=60^{\circ}C$, $p_{in}=14.7$ bar (R134a), 7.75 bar (R600a) and 25.995 bar (R404A). $\dot{m}_{in}=9$ kg/h.

Figure 7 shows the temperature, pressure and heat transfer coefficients distribution along the branch using three different fluids. As can be seen in the input data, the only difference between them is the inlet pressure. A significant temperature glide can be observed in figure 7a for the mixture; for the pure fluids temperatures differences are due to pressure drop and momentum changes along the two-phase flow region. Discontinuities of the heat transfer coefficient along condensing region, figure 7c, reveal the transition between annular to stratified flow.

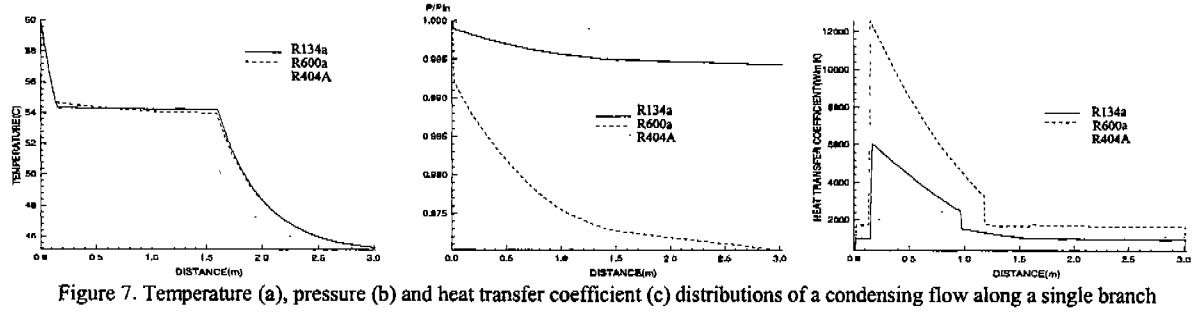


Figure 7. Temperature (a), pressure (b) and heat transfer coefficient (c) distributions of a condensing flow along a single branch

*Case 4*. Evaporation inside a branch with a sudden contraction in the inlet and a sudden enlargement in the outlet (fig. 4) using three different fluids. Input data: *i)* geometry: $D_{in}=D_{out}=5$mm, D=3mm, L=4m, $\theta=0$, $\zeta=1.5\text{x}10^{-6}$; *ii)* fluids: R134a, R600a (isobutane) and R404A; *iii)* tube wall boundary conditions: $T_{wall}=-10^{\circ}C$; *iv)* inlet fluid conditions (z=0): $x_{gin}=0.1$, $p_{in}=1.639$ bar (R134a), 0.887 bar (R600a) and 3.78 bar (R404A), $\dot{m}_{in}=0.9$ kg/h.

Figure 8 shows the temperature, pressure and heat transfer coefficients distribution along the branch using the three different fluids. Again temperature changes along the two-phase flow region are due to pressure drops, momentum variations and the kind of fluid (mixtures). Discontinuities of the heat transfer coefficient along the evaporating region, figure 8c, reveal the location of the dry-out point

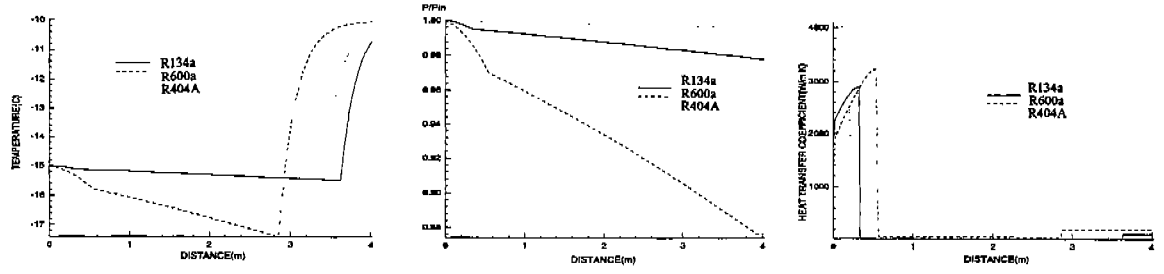


Figure 8. Temperature (a), pressure (b) and heat transfer coefficient (c) distributions of an evaporating flow along a single branch.

*Case 5*. An illustrative case of evaporation in parallel paths using a ternary mixture (R404A) is shown in figure 9. Input data: i) geometry: $D_{in}=D_{out}=12$ mm, $D_1=D_3=9$ mm, $D_2=10$ mm, L=6 m, $\theta=0$, $\zeta=1.5\text{x}10^{-6}$; iii) tube wall boundary conditions: $T_{wall1}=T_{wall2}=-5^{\circ}C$, $T_{wall3}=-1^{\circ}C$; iv) inlet fluid (z=0): $x_{gin}=0.25$, $p_{in}=3.74$ bar, $\dot{m}_{in}=144$ kg/h. As can be observed in figure 9, the thermal and fluid dynamic behaviour of the flow along the branches depend on the different wall boundary conditions and tube geometry. Dryout point can be located from the discontinuity in pressure distribution (after this point a nearly linear pressure distribution can be observed). The table below show some global values together with the mean outlet temperature and pressure.

Table 1. Global and local values of an evaporating flow along parallel branches

| BRANCH | mass flux(kg/h) | heat flux(W) | T(last vc of the branch) (°C) | $T_{out}$(°C) | $P_{out}$(bar) |
|---|---|---|---|---|---|
| 1 | 43.67 | 1787.56 | -9.97 | -9.71 | 3.61 |
| 2 | 57.47 | 2285.76 | -14.46 | -9.71 | 3.61 |
| 3 | 42.85 | 1834.58 | -2.54 | -9.71 | 3.61 |

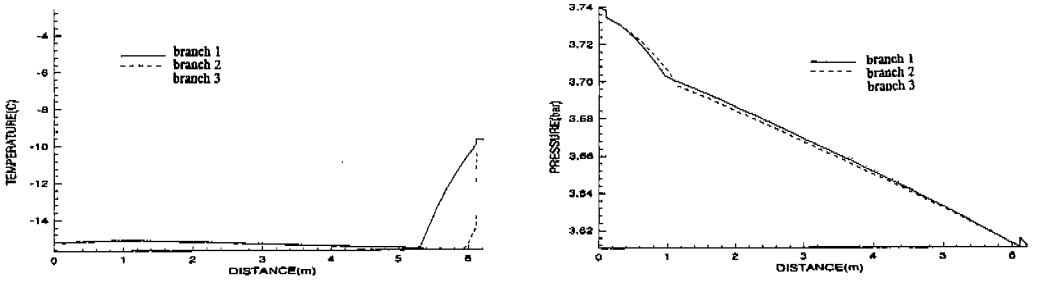


Figure 9. Temperature and pressure distribution of an evaporating flow through parallel branches.

## *CONCLUDING REMARKS*

A numerical study of condensation and evaporation inside ducts and using different refrigerant fluids (pure substances and mixtures) has been presented. Different numerical aspects related to the global algorithm (step by step method and pressure-based method), grid density, numerical schemes for the convection terms (first and higher order), and transition criteria have been presented. Even though the step by step method is much faster than the pressure-based algorithm, the latter is more general for the analysis of complex geometries and phenomena (reverse flow). For the analysed cases here presented, the higher order quick scheme gives a similar convergence rate than the first order uds and the second order smart scheme. Grid independent results are more easily obtained using the second transition criterion than the first one. The influence of the kind of fluid and geometry for evaporating and condensing flows has been shown. The software developed is general and flexible and its application for a specific condenser and evaporator is presented in a companion paper[23].

## *ACKNOWLEDGEMENTS*

This study has been supported by the Electrolux Compressors Companies - Spain and by the "Comisión Interministerial de Ciencia y Tecnologia" (TIC 95-0724).

## *REFERENCES*

1 Escanes, F., Pérez-Segarra C. D. and Oliva, A. (1995), Thermal and Fluid-Dynamic Behaviour of Double-Pipe Condensers and Evaporators. Int. J. of Num. Met. for Heat and Fluid Flow, Vol.5, No.9, pp.781-795.
4 Escanes, F., Pérez-Segarra C.D., Oliva, A. (1995), Numerical Simulation of Capillary Tube Expansion Devices, Int.J.Refr., Vol.18, No.2, pp.113-122.
2 Patankar, S. V. (1980), Numerical Heat Transfer and fluid flow, McGraw-Hill, New York, 1980.
3 Van Doormaal, J. P. And Raithby, G. D. (1994), Enhancements of the Simple Method for Predicting Incompressible Fluid Flows, Numerical Heat Transfer, vol. 7, pp.147-163.
5 REFPROP v.5.0 (Feb 1996), NIST Thermodynamic Properties of Refrigerants and Refrigerant Mixtures Database, Standard Reference Data Program, Gaithersbug, MD 20899, USA.
6 Gnielinski V. (1976), New Equations for Heat and Mass Transfer in Turbulent Pipe and Channel Flow, Int. Chem. Eng., vol.16, pp.359-368.
7 Lin S., Kwok, C. C. K., Li, R. Y., Chen, Z. H. and Chen, Z. Y. (1991),Local Frictional Pressure Drop During Vaporisation of R-12 Through Capillary Tubes, Int. J. Multiphase Flow, Vol.17, No.1, pp95-102.
8 Dobson, M.K., Chato, J.C., Wattelet, J.P. (1994), Heat Transfer and Flow Regimes During Condensation in Horizontal Tubes, ACRC TR-57.
9 Soliman, H. M. (1982), On the annular to wavy flow pattern transition during condensation inside horizontal tubes, The Canadian Journal of Chemical Engineering, 60, pp 475-481.
10 Rice, C. K. (1987), The Effect of Void Fraction Correlation and Heat Flux Assumption on Refrigerant Charge Inventory Predictions, ASHRAE Transactions, vol.93, pp.341-367.
11 Friedel L. (1979), Improved Friction Pressure Drop Correlation for Horizontal and Vertical Two-Phase Pipe Flow, European Two-Phase Flow Group Meeting, Ispra, Italy, Paper E2.
12 Frost, W., Dzanowic, G. S. (1967), An Extension of the Method of Predicting Incipient Boiling on Commercially Finished Surfaces, ASME/AIChe Heat Transfer Conf., paper 67-ht-61, 1-8.
13 Bergles, A.E., Rohsenow, W.M. (1964), The Determination of Forced-Conv. Surf.-Boiling Heat Tranfer, J. Heat Transfer, 86C, pp.365-372.
14 Forster, H. K., Zuber, N. (1955), Dynamics of Vapour Bubble Growth and Boiling Heat Transfer, AIChe J.1 no 4, pp. 531-535.
15 Saha, P., Zuber, N. (1974), Point of Net Vapour Generation and Vapour Volumetric Void Fraction, Proc. 15th Int. Heat Transfer Conf. Paper B4.7, pp175-179.
16 Hewitt, G. F. (1983), Gas-Liquid Flow , Heat Exchanger Design Handbook, sec.2.7.3, de. By E. U. Schlünder et al., Hemisphere Publishing Corporation, Washington.
17 Levy, S. (1967), Forced Convection Subcooled Boiling Prediction of Vapour Volumetric Frac., Int.J.Heat Mass Transfer, vol.10, pp.951-965.
18 Chen, J. C. (1966), Correlation for Boiling Heat Transfer to Saturated Fluids in Convective Boiling , I&EC Proc. Design & Dev., vol.5., no.3
19 Groeneveld, D. C. (1973), Post-Dryout Heat Transfer at Reactor Operating Conditions , Natl. Topical Meet. Water Reactor Safety, ANS paper AECL-4513, pp. 321-350, Utah.
20 Jung, D. S. and Radermacher R. (1993), Prediction of Evaporation Heat Transfer Coefficient and Pressure drop of Refrigerant Mixtures, Int. J. Refrigeration, Vol. 16, No.5, pp.330-338.
21 Hewitt, G. F. And Hall-Taylor, N. S. (1970), Annular Two-Phase Flow, Pergamon, Oxford.
22 Chisholm, D.(1969), Theoretical Aspects of Pressure Changes of Section during Steam-Water Flow, NEL Report 418.
23 J.Rigola, C.D.Pérez-Segarra, O.García-Valladares, J.M.Serra, M.Escribà, J.Pons, Numerical study and experimental validation of a complete vapour compression refrigerating cycle, Int. Compressor Eng. Conference, Purdue University, 1998.